# Quasi-reflected Interface Conditions for Variational Nodal Lattice Calculations

E. E. Lewis[1], M. A. Smith[2] and G. Palmiotti[2]
[1]Northwestern University, Department of Mechanical Engineering, Evanston, Illinois 60208
[2]Argonne National Laboratory, 9700 South Cass Avenue, Argonne, Illinois 60439

Quasi-reflected interface conditions are formulated to partially decouple periodic lattice effects from the pin-cell to pin-cell flux variation in the finite subelement form of the variational nodal code VARIANT. With fuel-coolant homogenization eliminated, the interface variables that couple pin-cell sized nodes are divided into low-order and high-order spherical harmonic terms, and reflected interface conditions are applied to the high-order terms. This approach dramatically reduces the dimension of the resulting response matrices and leads to sharply reduced memory and CPU requirements for the solution of the resulting response matrix equations. The method is applied to a two-dimensional OECD/NEA PWR benchmark containing MOX and $UO_2$ fuel assemblies. Results indicate that the quasi-reflected interface conditions result in very little loss of accuracy relative to the corresponding full spherical harmonics expansion.

***KEYWORDS: neutron transport, variational nodal method, spherical harmonics, lattice cell, homogenization.***

## 1. Introduction

The long-standing approach to LWR physics has been to homogenize cross sections using lattice code calculations at the fuel assembly level before performing whole-core diffusion calculations. While such methods have been successfully fine-tuned for the treatment of existing reactor cores, the homogenization and subsequent dehomogenization procedures require discontinuity factors or other equivalency techniques that are error-prone, particularly when adjoining lattice cells have distinctly different fuel compositions.

Under OECD/NEA auspices, a benchmark problem without spatial homogenization of fuel and coolant [1] was developed based upon a four assembly pressurized water reactor configuration to test and compare state-of–the–art transport codes. Among the insights gained from the benchmarking exercise was that very high-order angular approximations are required to achieve acceptable accuracy [2]. With the subelement formulation of the variational nodal code VARIANT [6], for example, as high as $P_{13}$, spherical approximations were required to obtain benchmark quality results [3]. The need for high-order angular approximations make the application of present-generation transport codes to large scale problems (such as a PWR core) both prohibitively expensive in CPU time and dauntingly demanding in memory requirements.

The objective of this work is to reduce the memory and CPU time requirements of the subelement form[3] of VARIANT [4-6] without a commensurate loss of accuracy. We

accomplish this by tailoring the spherical harmonics expansions with quasi-reflected interface conditions that partially decouple the periodic lattice effects from the pin-cell to pin-cell variation in the flux. We divide the interface variables that couple the pin-cell nodes in VARIANT into low-order and high-order angular components of the spherical harmonics expansion. Reflected boundary conditions are applied to the high-order terms while the low order terms are maintained for nodal coupling. The resulting response matrix dimensions are substantially reduced since only the low-order terms of the spherical harmonics expansion remain as interface variables. We do not believe these modifications to the spherical harmonic expansion will introduce significant error.

In the following section we formulate the subelement form of the variational nodal method to include the quasi-reflected interface conditions. In section 3 we apply the new method to a simple seven-group four pin-cell problem in which MOX and $UO_2$ fuel pins occupy adjoining positions. We then use the method to solve the two-dimensional form of the OECD/NEA benchmark problem, comparing errors against a Monte Carlo reference solution, and examining CPU times. We conclude with a discussion of possible future directions.

## 2. Formulation

The formulation of the quasi-reflected interface conditions begins with the discretized functional for the subelement form of the variational nodal method [3]**:**

$$F_v[\boldsymbol{\xi},\boldsymbol{\chi}] = \boldsymbol{\xi}^T \mathbf{A}\boldsymbol{\xi} - 2\boldsymbol{\xi}^T \mathbf{q} + 2\boldsymbol{\xi}^T \mathbf{M}\boldsymbol{\chi} \tag{1}$$

and

$$F[\boldsymbol{\xi},\boldsymbol{\chi}] = \sum_v F_v[\boldsymbol{\xi},\boldsymbol{\chi}], \tag{2}$$

where each heterogeneous node, $V_v$, corresponds to one fuel-pin cell. Within each node even-parity spherical harmonics in angle are combined with finite elements in space. Odd-parity spherical harmonics and spatial orthogonal polynomial trial functions are used along the interfaces. The matrices **A** and **M** and the group source vector **q** result from integrals of the trial functions. $\boldsymbol{\xi}$ and $\boldsymbol{\chi}$ are the unknown even- and odd-parity coefficient vectors. Requiring this functional to be stationary with respect to variations in $\boldsymbol{\xi}$ and $\boldsymbol{\chi}$, yields the system of equations for the even-parity flux coefficients within the node,

$$\mathbf{A}\boldsymbol{\xi} = \mathbf{q} - \mathbf{M}\,\boldsymbol{\chi}, \tag{3}$$

and the requirement that

$$\boldsymbol{\varphi} = \mathbf{M}^T \boldsymbol{\xi} \tag{4}$$

be continuous across the interfaces.

Suppose we partition $\boldsymbol{\varphi}$ and $\boldsymbol{\chi}$ into three parts. Let the subscript *l* denote the low angular order terms; say the $P_1$ terms or the $P_1$ through $P_3$ terms. The higher-order terms are divided into contributions from the $Y_{lm}(\hat{\Omega})$ spherical harmonics with even *m* (subscript *e*) and odd *m* (subscript *o*). Thus we have

$$\boldsymbol{\chi} = \begin{bmatrix} \boldsymbol{\chi}_l \\ \boldsymbol{\chi}_e \\ \boldsymbol{\chi}_o \end{bmatrix} \quad \boldsymbol{\varphi} = \begin{bmatrix} \boldsymbol{\varphi}_l \\ \boldsymbol{\varphi}_e \\ \boldsymbol{\varphi}_o \end{bmatrix} \tag{5}$$

Making the corresponding partition of the $\mathbf{M}$ matrix, $\mathbf{M} = \begin{bmatrix} \mathbf{M}_l & \mathbf{M}_e & \mathbf{M}_o \end{bmatrix}$, Eq. (3) becomes

$$\mathbf{A}\boldsymbol{\xi} = \mathbf{q} - \mathbf{M}_l\boldsymbol{\chi}_l - \mathbf{M}_e\boldsymbol{\chi}_e - \mathbf{M}_o\boldsymbol{\chi}_o . \tag{6}$$

Similarly, the even-parity surface moments of Eq. (4) are given as

$$\boldsymbol{\varphi}_l = \mathbf{M}_l^T\boldsymbol{\xi} \tag{7a}$$

$$\boldsymbol{\varphi}_e = \mathbf{M}_e^T\boldsymbol{\xi} \tag{7b}$$

$$\boldsymbol{\varphi}_o = \mathbf{M}_o^T\boldsymbol{\xi} \tag{7c}$$

We next apply reflected interface conditions to the higher-order angular terms thereby decoupling them from adjoining nodes. In other work [7], the reflected conditions have been shown to set $\boldsymbol{\chi}_e = \mathbf{0}$ and $\boldsymbol{\varphi}_o = \mathbf{0}$. Implementing these rules in Eq. (6) yields

$$\mathbf{A}\boldsymbol{\xi} = \mathbf{q} - \mathbf{M}_l\boldsymbol{\chi}_l - \mathbf{M}_o\boldsymbol{\chi}_o . \tag{8}$$

We can solve for $\boldsymbol{\xi}$ and apply Eq. (7a) to obtain

$$\boldsymbol{\varphi}_l = \mathbf{M}_l^T\mathbf{A}^{-1}\mathbf{q} - \mathbf{M}_l^T\mathbf{A}^{-1}\mathbf{M}_l\boldsymbol{\chi}_l - \mathbf{M}_l^T\mathbf{A}^{-1}\mathbf{M}_o\boldsymbol{\chi}_o . \tag{9}$$

Applying Eq. (7c) and setting $\boldsymbol{\varphi}_o = \mathbf{0}$ yields

$$\mathbf{0} = \mathbf{M}_o^T\mathbf{A}^{-1}\mathbf{q} - \mathbf{M}_0^T\mathbf{A}^{-1}\mathbf{M}_l\boldsymbol{\chi}_l - \mathbf{M}_o^T\mathbf{A}^{-1}\mathbf{M}_o\boldsymbol{\chi}_o . \tag{10}$$

Eliminating $\boldsymbol{\chi}_o$ between Eqs. (9) and (10) yields an expression for the low-order even-parity surface moments in terms of the group source and the low-order odd-parity surface moments:

$$\boldsymbol{\varphi}_l = \mathbf{C}_l\mathbf{q} - \mathbf{G}_l\boldsymbol{\chi}_l , \tag{11}$$

where

$$\mathbf{C}_l = \mathbf{M}_l^T\mathbf{A}^{-1} - \mathbf{M}_l^T\mathbf{A}^{-1}\mathbf{M}_o\left(\mathbf{M}_o^T\mathbf{A}^{-1}\mathbf{M}_o\right)^{-1}\mathbf{M}_o^T\mathbf{A}^{-1} \tag{12}$$

and

$$\mathbf{G}_l = \mathbf{M}_l^T\mathbf{A}^{-1}\mathbf{M}_l - \mathbf{M}_l^T\mathbf{A}^{-1}\mathbf{M}_o\left(\mathbf{M}_o^T\mathbf{A}^{-1}\mathbf{M}_o\right)^{-1}\mathbf{M}_o^T\mathbf{A}^{-1}\mathbf{M}_l . \tag{13}$$

Finally, making the linear transformation $\mathbf{j}_l^{\pm} = \tfrac{1}{4}\boldsymbol{\varphi}_l \pm \tfrac{1}{2}\boldsymbol{\chi}_l$, we obtain the low-order response matrix equations in the form $\mathbf{j}_l^{+} = \mathbf{R}_l\mathbf{j}_l^{-} + \mathbf{B}_l\mathbf{q}$.

## 3. Results

The quasi-reflected interface approximation has been applied to a test problem consisting of four water-reactor pin-cells in a checkerboard pattern with reflected conditions on the outer boundaries. Two cells contain 8.7% MOX fuel and two contain $UO_2$ fuel. The seven-group cross sections and the cell geometries are the same as those specified for the recent OECD/NEA benchmarking exercise [1]. For the four cell problem a 25 point grid of linear triangular finite elements specifies the fuel-coolant interface, and the interface trial functions are linear in space. To solve this test problem we wrote a

prototype code in MathCAD. We refer to the tailored spherical harmonic expansions hereafter as $P_{M\text{-}N}$, where the high-order base approximation in the node interior is order $M$ and the interface coupling is order $N$. In this paper $P_{11}$, is used for all high-order base expansions, and thus we employ $P_{11\text{-}N}$ approximations.

In Table 1 we tabulate results for the four cell problem: the multiplication, the percent error relative to the reference $P_{11}$ result, and the dimension of the response matrix for each set of angular trial functions. Standard $P_N$ calculations are included for comparison. Note that the $P_{11\text{-}1}$ approximation is roughly as accurate as the $P_9$ calculation even though its response matrix dimension is only 1/25 of that of the $P_9$ matrix. Also, the $P_{11\text{-}3}$ approximation comes very close to the $P_{11}$ accuracy even though its response matrix dimension is only 1/9 of that of the $P_{11}$ matrix.

**TABLE 1 Eigenvalue Comparisons for a Four Pin-cell Benchmark**

| | Multiplication Constant | Error (%) | R matrix Dimension |
|---|---|---|---|
| $P_1$ | 1.217708 | 0.336 | 8 |
| **$P_{11\text{-}1}$** | **1.220934** | **0.027** | **8** |
| $P_3$ | 1.218931 | 0.191 | 32 |
| **$P_{11\text{-}3}$** | **1.221398** | **0.011** | **32** |
| $P_5$ | 1.219857 | 0.115 | 72 |
| $P_7$ | 1.220503 | 0.062 | 128 |
| $P_9$ | 1.220941 | 0.027 | 200 |
| $P_{11}$ | 1.221266 | - | 288 |

To allow treatment of larger, more realistic configurations, we have incorporated the new formalism into the two-dimensional form of VARAINT-SE, the finite subelement form of VARIANT. The coding was first verified by treating single cells with reflected boundary conditions. In these and subsequent calculations we employed the finite element mesh of quadratic isoparametric finite elements shown in Figure 1, where each node corresponds to a single pin-cell. The odd-parity Lagrange multipliers along the interfaces are quadratic in space. A five-region lumped-source approximation is used in each cell.

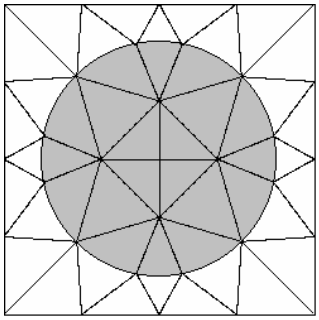

**Figure 1. Quadratic Finite Element Mesh for a Pin-cell**

We have applied the new method to the seven energy-group, four fuel assembly OECD/NEA PWR benchmark problem shown in Figure 2. When fuel-water homogenization is eliminated, earlier calculations have shown that very high order angular approximations are required to achieve reasonable agreement with multigroup Monte Carlo results. Table 2 shows percent errors for the multiplication and power distribution relative to a precise multigroup Monte Carlo solution. The Monte Carlo reference values with 68% confidence intervals are $1.18655 \pm 0.003$ for the eigenvalue and $2.498 \pm 0.07$ for the maximum pin power, with the mean pin power normalized to one. The $P_{11\text{-}N}$ approximations converge towards the $P_{11}$ approximation, with some of the residual errors relative to the Monte Carlo solution being attributable to the error remaining in the $P_{11}$ approximation itself. This may be confirmed by employing the $P_{11}$ solution as the reference as we have done in Table 3.

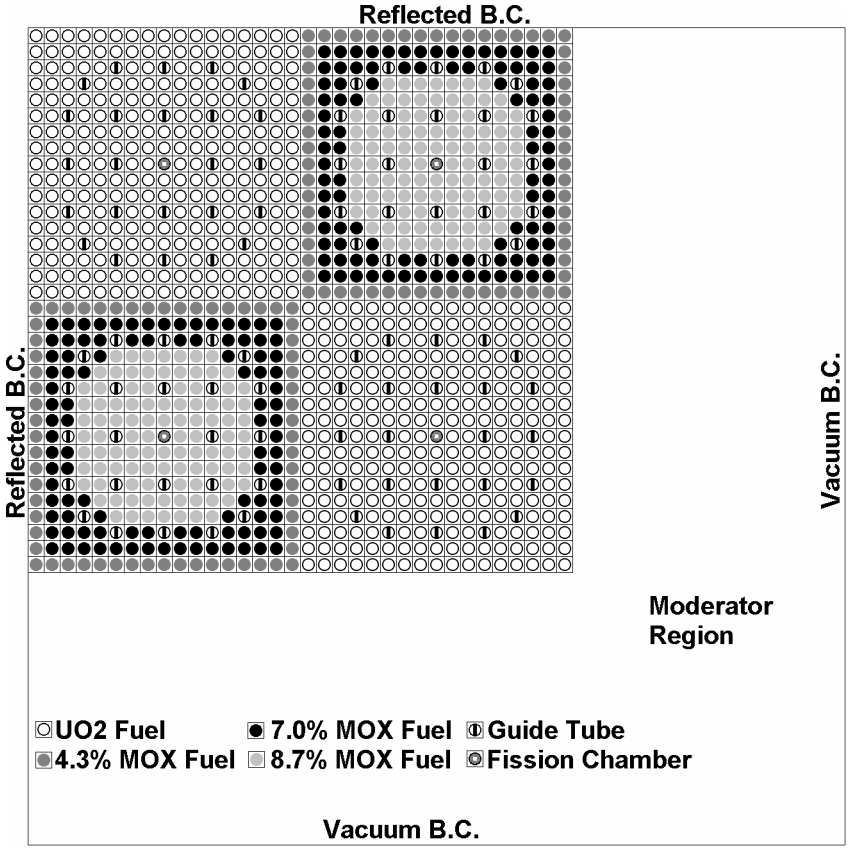


**Figure 2 OECD/NEA Two-Dimensional Benchmark configuration**

Table 4 provides timing comparisons made on Sun-60 Sparc Stations. The MCNP Monte Carlo reference calculation required approximately one week of CPU time. The VARIANT CPU times are divided between response matrix formation and solution though standard outer iteration on the fission source. In these calculations no acceleration was applied to the inner iterations. As indicated, replacing $P_{11}$ by $P_{11\text{-}N}$ approximations reduces the solution time by over an order of magnitude in all cases presented. We also found that the solution times for $P_N$ and $P_{11\text{-}N}$ are virtually identical, as expected. The $P_{11\text{-}N}$ response matrix formation times are moderately larger than for $P_{11}$ as a result of the

additional matrix manipulation required. Since the response matrices must be formed for each node type, in this case seven, it dominates the CPU time. As indicated in the discussion, however, in the future this difficulty may be circumvented.

**Table 2 Percent Error for Two-Dimensional Benchmark Compared to Monte Carlo Reference**

| | Eigenvalue k | Maximum Pin Power | Pin Power Maximum | Pin Power RMS |
|---|---|---|---|---|
| $P_1$ | -0.276 | 1.013 | 5.881 | 1.758 |
| **$P_{11-1}$** | **-0.037** | **0.871** | **2.543** | **0.829** |
| $P_3$ | -0.318 | 1.228 | 2.194 | 1.043 |
| **$P_{11-3}$** | **-0.062** | **0.045** | **0.767** | **0.222** |
| $P_5$ | -0.309 | 0.897 | 1.719 | 0.751 |
| **$P_{11-5}$** | **-0.077** | **0.063** | **0.801** | **0.238** |
| $P_{11}$ | -0.090 | 0.060 | 0.799 | 0.243 |

**Table 3 Percent Error for Two-Dimensional Benchmark Compared to P11 Reference**

| | Eigenvalue k | Maximum Pin Power | Pin Power Maximum | Pin Power RMS |
|---|---|---|---|---|
| $P_1$ | -0.186 | 0.952 | 5.646 | 1.723 |
| **$P_{11-1}$** | **0.054** | **-0.931** | **2.915** | **0.880** |
| $P_3$ | -0.228 | 1.227 | 1.819 | 0.912 |
| **$P_{11-3}$** | **0.028** | **-0.015** | **0.274** | **0.076** |
| $P_5$ | -0.219 | 0.818 | 1.180 | 0.600 |
| **$P_{11-5}$** | **0.013** | **0.003** | **0.204** | **0.065** |
| $P_{11}$ | - | - | - | - |

**Table 4 Computing Time for Two-Dimensional Benchmark CPU (hrs.)**

| | R Matrix Formation Per node type | Outer Iterations: Solution |
|---|---|---|
| $P_{11-1}$ | 3.40 | 0.22 |
| $P_{11-3}$ | 3.24 | 0.60 |
| $P_{11-5}$ | 3.09 | 1.46 |
| $P_{11}$ | 2.47 | 25.60 |

## 4. Discussion

The preceding sections present a new approach for coupling lattice to whole-core transport calculations in a consistent manner while at the same time eliminating the need for fuel-coolant homogenization. The variation nodal method upon which the technique is based divides transport calculations into first forming response matrices, and then solving the resulting equations. The new approach greatly reduces the solution time, without a substantial loss in accuracy, but it does significantly increase the CPU time devoted to response matrix formation. Thus while response matrix formation accounts for about 40 percent of the $P_{11}$ CPU time in the benchmark problem, it dominates the faster $P_{11\text{-}N}$ calculations.

We envision two approaches used separately or in combination to circumvent this difficulty. First, the integral form of the variational nodal method has been shown to greatly reduce both CPU time and memory required to form response matrices [8]. Moreover, the integral formulation appears to be compatible with the tailored spherical harmonic approach. Memory as well as CPU time reductions are important for they allow higher-order spherical harmonics expansions to be contained within a workstation memory. Second, response matrix formations for different node types are entirely independent from one another. Thus with the employment of master-slave message passing algorithms, the response matrices can be formed in parallel on a workstation cluster.

We also believe that there may be significant potential in generalizing the tailored spherical harmonics methods to three dimensions. In two-dimensional spherical harmonics calculations we use only the cosine series, that is the $Y_{lm}$, $m \le l$, with only nonnegative values of $m$. In three-dimensional calculations the sine series, that is the negative values of $m$, are also present. The lattice effects that require high-order angular approximation, and which we treat with quasi-reflected interface conditions, occur predominately in the X-Y plane. Therefore it seems that by adding only the low–order sine terms to the expansion the tailored spherical harmonics methodology can be incorporated into the three-dimensional form of VARIANT-SE to substantially reduce the effort required to perform whole-core transport calculations into which lattice effects have been effectively incorporated.

## Acknowledgements

This work was supported by the U.S. Department of Energy under Contract numbers DE-FG07-01ID1410 and W-31-109-Eng-38.

## References

(1) E. E. Lewis, G. Palmiotti, T. A. Taiwo, R. N. Blomquist, M. A. Smith and N. Tsoulfanidis, Benchmark Specification for Deterministic 2-D/3-D MOX Fuel

Assembly Transport Calculations without Spatial Homogenization (C5G7 MOX), *NEA/NSC/DOC(2001)4*, March, 2001.

(2) M. A. Smith, E. E. Lewis and Byung-Chan Na, "Benchmark on Deterministic 2-D MOX Fuel Assembly Transport Calculations without Spatial Homogenization," *Prog. Nucl. Energy*, **45**, 107-118 (2004)

(3) M. A. Smith, N. Tsoulfanidis, E. E. Lewis, G. Palmiotti, and T. A. Taiwo, "A Finite Subelement Generalization of the Variational Nodal Method," *Nucl. Sci. Eng*. **144**, 36 (2003).

(4) C. B. Carrico, E. E. Lewis and G. Palmiotti, "Three-Dimensional Variational Nodal Transport Methods for Cartesian, Triangular and Hexagonal Criticality Calculations," *Nucl. Sci. Eng.,* **111**, 168-179 (1992).

(5) G. Palmiotti, C. B. Carrico, and E. E. Lewis, "Variational Nodal Transport Methods with Anisotropic Scattering," *Nucl. Sci. Eng.,* **115**, 223 (1993).

(6) G. Palmiotti, E. E. Lewis and C. B. Carrico, VARIANT: VARIational Anisotropic Nodal Transport for Multidimensional Cartesian and Hexagonal Geometry Calculation, ANL-95/40 Argonne National Laboratory, 1995.

(7) E. E. Lewis, C.B. Carrico and G. Palmiotti, "Variational Nodal Formulation for the Spherical Harmonics Equations," *Nucl. Sci. Eng.*, **122**, 194 (1996).

(8) M. A. Smith, G. Palmiotti, E. E. Lewis, and N. Tsoulfanidis, "An Integral Form of the Variational Nodal Method," *Nucl. Sci. Eng.* **146**, 141 (2004).